Tsunami Inundation Modeling of Sequim Bay Area, Washington, USA from a Mw 9.0 Cascadia Subduction Zone Earthquake

Chun-Juei Lee

A report prepared in partial fulfillment of
the requirements for the degree of

Master of Science
Earth and Space Sciences: Applied Geosciences

University of Washington

June 2017

Project mentor:
Recep Cakir, Washington Department of Natural Resources

Internship coordinator:
Kathy Troost

Reading committee:
Juliet G. Crider
Randall J. LeVeque

MESSAGe Technical Report Number: 057

Abstract

The Strait of Juan de Fuca and the coastline nearby are prone to tsunami attacks along the Cascadia Subduction Zone (CSZ). Besides the tsunami deposits that exist on the outer coast, the inland geological evidence shows that nine sandy-muddy Cascadia tsunami deposits intrude a 2500-yr-old sequence of peat deposits beneath a tidal marsh at Discovery Bay, Northern Olympic Peninsula, Washington (Williams et al., 2005). Thus, assessing the potential damage for the next CSZ earthquake tsunami event is important. In this study, I conducted tsunami simulations using the GeoClaw numerical model by a scenario earthquake. The earthquake scenario adopted for this study is a Mw 9.0 CSZ earthquake, also known as the "L1" scenario (Witter et al., 2011). Fine-resolution (1/3 arc-second) digital elevation models (DEMs) are used to provide high resolution tsunami inundation results on Sequim Bay area at northern Olympic Peninsula. The numerical gauges which are set around the major Infrastructure and properties provide information of wave height, wave velocity and wave arrival time. Four tsunami waves with 2-meter-height are found over the ten hours simulation. Also, two spits at the entrance of Sequim Bay can diminish and delay the tsunami impacts in the Bay. The modeling results will contribute to public safety administration in the Pacific Northwest as an aid to development of hazard mitigation plans and emergency response.

Table of Contents

List of Figures

Acknowledgments

I would like to thank Washington State Department of Natural Resources for giving me an intern opportunity in the summer of 2016. I would also like to thank Recep Cakir for mentoring me during the summer time in DNR. I also thank Kathy Troost for coordinating the intern project and introducing me to DNR.

I would also like to thank Carrie Garrison-Laney, Timothy Walsh and Frank Gonzalez for sharing me wealth knowledge on tsunami deposits and tsunami impacts around Puget Sound.

Finally, I would like to acknowledge my reading committee and the MESSAGe program. Thanks to Randall LeVeque and Loyce Adam for guiding me operating the tsunami model and sharing me knowledge of tsunami dynamic. I would also like to acknowledge Juliet Crider for guiding me finish this report, providing reference for geological background, correcting my first draft and encouraging me for doing more detailed studies.

1.0 Introduction:

While no earthquakes with magnitude larger than 7.5 have been observed in the State of Washington during the past 150 years, the Cascadia Subduction Zone (CSZ) has potential to produce mega-earthquakes with magnitude larger than 9, and these earthquakes are likely to trigger tsunamis (Hopper et al., 1975; Heaton and Hartzell, 1987). Geological evidence found in the outer coast of Washington and in tidal marshes along the Strait of Juan de Fuca showed that at least seven mega-earthquake events have occurred within 2500 years (Atwater, 1987; Williams et al., 2005) with a return interval of 400-600 years. The last event occurred in A.D. 1700, generating a tsunami that was not only recorded in the native American's oral history but also spread across the Pacific Ocean to be documented in Japanese literature (Atwater et al., 2005). Therefore, the CSZ is expected to generate destructive tsunamis that will impact the Pacific Northwest in the future. The Pacific Northwest is one of the areas in the world with both a large earthquake potential and heavily populated urban centers. Thus, the investigation of tsunami impacts from mega-earthquakes across the Pacific Northwest is important.

The characteristics of tsunamis change with bathymetry. Previous studies have described the behavior tsunami waves in detail (Dean and Dalrymple, 1991). For example, the wavelength of a tsunami is much larger than the water depth in the ocean. When the tsunami waves travel in deep water, the velocity of the tsunami wave is proportional to the square root of water depth. Then, when the tsunami waves arrive at shallow water, the velocity decreases and the amplitude increases. Also, the tsunami waves undergo shoaling, refracting, reflection and diffraction (Murata et al., 2010). To model these tsunami characteristics, previous studies found the non-linear shallow-water approximations of Navier-Stokes equations worked well to describe tsunami behavior in the open ocean, on continent shelves, and around the shoreline (Liu et al., 2008; Mader, 1988).

For this study, I focused on tsunami simulation at Sequim Bay in Clallam County, Washington, United States. Sequim Bay is located inside Puget Sound on the Olympic Peninsula (Figure 1).

The study area is close to Discovery Bay, where the tsunami deposits are well-documented (Williams et al., 2005). However, the tsunami hazards and related deposits in Sequim Bay have not been identified. Previous studies include a series of tsunami hazard maps that have been prepared for coastal communities on the Olympic Peninsula (Geist, E. L., 2005; Walsh et al., 2002a; Walsh et al., 2002b). Nevertheless, detailed numerical simulation in Sequim Bay has not previously been published. In collaboration with the Washington State's Department of Natural Resources, I conducted a tsunami simulation with 1/3 arc –second (10 meters) resolution to calculate the wave propagation and inundation in Sequim Bay. Additionally, my study provided an opportunity to identify possible locations to find tsunami deposits.

In order to run the model, I compiled: a 10-meter DEMs with bathymetry around Sequim Bay; 1-minute DEMs with offshore bathymetry; and a rupture model for the Mw 9.0 earthquake source. Due to lack information about the focal mechanism and sea floor deformation of the CSZ events, studies have used hypothetical scenarios to assess tsunami hazards along the coast (Witter et al., 2011). Previous studies developed the tsunami scenarios from the knowledge of the structure of the Cascadia mega-thrust (Goldfinger, 1994; McCrory et al., 2004). I selected the L1 scenario for an Mw 9.0 earthquake, which is one of the 15 scenarios developed by Witter et al. (2011) to conduct the tsunami simulation.

2.0 Background:

2.1 Cascadia subduction zone

The plate tectonic and associated geological activity in the Pacific Northwest is complicated. The Juan de Fuca Plate is subducting under the North American plate at ~4 centimetres per year, producing the Cascadia Subduction Zone (CSZ), which is a 1000 km long megathrust fault that stretches from Northern Vancouver Island to Cape Mendocino California (Heaton and Hartzell, 1985; Morey et al., 2013). During a megathrust earthquake on the CSZ, broad-scale movement of the seafloor would uplift the seawater and create a tsunami. The geological evidence for the last CSZ earthquake and tsunami (in 1700) has been well-studied (Satake et al., 1996; Atwater

et al., 2005; Williams et al., 2005; Kilfeather et al., 2007). Petersen et al. (2002) predict a 10 to 14 percent chance that the next event would happen in the next 50 years.

2.2 Bathymetry and Topography in Sequim bay

Sequim Bay is located in the northeastern of the Olympic Peninsula. It is connected to the Strait of Juan de Fuca and is almost enclosed by two large sand spits, Travis and Gibson spits. (Figure 2). The bay is approximately 3.5 miles in length and over a mile wide. The bathymetry of Sequim bay drops off rapidly from the entrance. The deepest area in the bay is about 38 meters, while the shallowest areas are located at the south end near the village of Blyn (Elwha-Dungeness Planning Unit, 2005). The geomorphology of Sequim Bay is shaped by glacier activity more than fluvial activity. The coastal geology of Sequim Bay is dominated by glacial till and glacial outwash, with alluvial deposits occurring at the head of the bay and where small streams enter the bay (Schasse, 2003). Coastal bluffs are the major geomorphic feature of the interior bay. The spatial and temporal distribution of the bluff recession might be affected by wave, wind and precipitation.

Gibson and Travis sand spits are two major features that impact the morphology and hydrodynamics of the bay. Travis Spit is nearly a mile in length and was formed by longshore drift derived from bluffs located to the east of the Strait (Todd et al., 2006). Travis Spit is a barrier which helps protect the inner bay from waves. On the other hand, Gibson Spit is about 0.9 mile in length formed by sediments transport from bluff erosion along the drift cell located northwest of Sequim bay (Todd et al., 2006). Also, a relatively smaller spit is located near the south end of Gibson spit. By protecting the mouth of Bell Creek from waves and wind, Gibson Spit and the smaller spit help to develop a tidal lagoon inside the spit. In addition, near the entrance of Gibson Spit, Bell Creek Valley leads to the city of Sequim. The tidal lagoon area near the entrance of the valley is called The Lagoon, a natural saltwater lagoon adjoining to the Strait of Juan de Fuca (Figure 3).

2.3 Tsunami deposits

Tsunami deposits have been found in Discovery Bay at the south shore of the Strait of Juan de Fuca, just a few miles east of Sequim Bay (Figure 1). Nine muddy sand beds interrupt a 2500-yr-old sequence of peat deposits beneath a tidal marsh at the head of Discovery Bay (Williams et al., 2005). Although Sequim Bay is located near Discovery Bay, no studies of tsunami deposits have been conducted in Sequim Bay. Historical maps from 1870 showed coast of Sequim Bay has not changed too much, except for slight differences in the Lagoon area (The Puget Sound River History Project). Some historical lagoon and tidal marsh has been eliminated by fill or has been disturbed for construction (Todd et al., 2006). The sedimentary environment may not be suitable for preservation of tsunami deposits, but my study provides an overlook of potential locations to find tsunami deposits.

2.4 Tsunami Vulnerability of city of Sequim and Sequim Bay

The Sequim Bay area faces hazards from two types of tsunami sources: distant Pacific Rim earthquakes and earthquakes on the Cascadia Subduction Zone. Between these, earthquakes on the Cascadia Subduction Zone are considered to be more hazardous, potentially causing more damage than other distant earthquakes. Inundations are highly expected during CSZ tsunami events.

The coast area around Sequim Bay and Bell Creek Valley may be vulnerable to inundation. Facilities along the shoreline of Sequim Bay include a federal marine sciences laboratory, a state park, a marina, businesses run by the Jamestown S'Klallam Tribe, and a number of other private homes and tourist facilities. A previous study indicated only 1% of Sequim businesses are located within the tsunami hazard zone, but the sales volume of these business is more than $3.8 million (Wood and Soulard, 2008). Also, a section of Highway 101 was built near the tsunami inundation area where is close to the bottom of the bay.

2.5 Inundation modeling

Inundation modeling studies can evaluate the tsunami generation, wave propagation and inundation potential for this study area. Available modeling tools take different approaches to

solving the physical problem. Several models solve the depth-integrated and long-wave based equations. For instance, CoulWave (Lynett et al., 2002) and Funwave (Kirby et al., 1998) solve Boussinesq equation for the tsunami waves propagation. In contrast, COMCOT (Liu et al, 1998), MOST (Titov and Gonzalez, 1997) and GeoClaw (LeVeque et al., 2011) solve the shallow water equations. While many tools have the ability to simulate the tsunami dynamics, the goal of this study was to solve the tsunami propagation and inundation problem in the Sequim Bay area. Although the Boussinesq models solve the weak dispersive waves that increase the accuracy of short-waves, the computational cost is higher than shallow water equation models. Thus, I adopted a model that will provide an acceptable accuracy with low computational time and cost. In this case, the two-dimensional depth-integrated shallow water equation models were the simplest solution. Therefore, this study uses Geoclaw for the tsunami modeling, an open-source software as part of Clawpack (Clawpack Development Team, 2017). Geoclaw has been widely used for tsunami hazard assessment in previous studies. For example, the model was adapted to analyze the Probabilistic Tsunami Hazard Assessment (PTHA) in Washington and California (Gonzalez et al., 2013a; Gonzalez et al., 2013b), and other tsunami hazard assessment in New Zealand (Hayes et al., 2010; Borerro et al., 2015). In addition, the model had been used to analyze the reginal impact caused by 2011 Japan tsunami and 2010 Chile tsunami event (Zhang et al., 2011; Yu et al., 2011). Furthermore, the validation against tide gauges showed the model performs well in tsunami propagation in the ocean (Arcos and LeVeque, 2015). The current code was approved by the U.S. National Tsunami Hazard Program for the modeling work after against benchmark problems (Gonzalez et al., 2011).

2.6 Data sources

Digital Elevation Models:

The tsunami model requires the topography and bathymetry of the model area. The 1/3 arc-seconds (~10 meters) digital elevation models (DEMs) from NOAA's National Geophysical Data Center (NGDC) were used in this study. The DEMs used in this study are developed for the National Tsunami Hazard Mitigation Program (NTHMP). These DEMs were referenced to the vertical tidal datum of Mean High Water (MHW) and horizontal datum of World Geodetic

System 1984 geographic (WGS 84) (Carignan, 2014). The 1-minute ETOPO1 global relief model are also used in the model to cover the whole computational domain (Amante and Eakins, 2009).

GIS database:

The base zonal map and building inventory of the Sequim Bay area from Washington Department of Natural Resources were used in ArcGIS. The information of building inventory included estimated value, building date, and building material. The value of properties was used to estimate the potential cost of damage due to inundation.

3.0 Methods:

3.1 Geoclaw

GeoClaw is a specialized version of Clawpack that has been modified to deal with tsunami simulation (Clawpack Development Team, 2017). The model uses the finite-volume method to solve both linear and non-linear shallow water equations. Adaptive mesh refinement (AMR) enables the model to deal with different scales of the problem: the broad, regional scale for tsunami source, and higher-resolution, local topography for the specific study area. Major algorithmic and software design contributions have been made by Randall J. LeVeque and collaborators at the University of Washington.

3.2 Equations

The propagation of tsunami waves can be described by shallow water equations because the wavelength is much greater than the water depth. The following two-dimensional non-linear shallow water equation is solved in Geoclaw (LeVeque et al., 2011):

$$h_t + (hu)_x + (hv)_y = 0$$

$$(hu)_t + (hu^2 + \frac{1}{2}gh^2)_x + (huv)_y = -ghB_x$$

$$(hv)_t + (huv)_x + (hv^2 + \frac{1}{2}gh^2)_y = -ghB_y$$

where $u(x, y, t)$ and $v(x, y, t)$ are depth-averaged horizontal velocity; x and y are the horizontal coordinates; and h is the fluid depth. The relationship between water surface elevation and fluid depth is $\eta(x, t) = h(x, t) + B(x, t)$. $B(x, y, t)$ is the bathymetry. g is the gravitational acceleration.

When tsunami waves arrive at the shoreline, a drag coefficient $D(h, u, v)$ is added to the momentum equation to describe the bottom friction term for calculating the inundation. The two-dimension non-linear shallow water equation then becomes:

$$(hu)_t + (hu^2 + \frac{1}{2}gh^2)_x + (huv)_y + ghB_x = -D(h, u, v)hu$$
$$(hv)_t + (huv)_x + (hv^2 + \frac{1}{2}gh^2)_y + ghB_x = -D(h, u, v)hv$$
$$D(h, u, v) = n^2 g h^{-7/3} \sqrt{u^2 + v^2}$$

where n is the Manning coefficient that depends on the roughness. The value of n = 0.025 is often used. The detailed numerical algorithm can be found in the Geoclaw package (LeVeque et al., 2011).

3.3 Numerical Setting: Domain, boundary condition and numerical grid

The computational domain extends from longitude 128.5W to 122.1W and latitude 45.42S to 51.02S. Six regions in the computational domain are developed to describe finer resolution. The first region contains all the areas of interest, which includes the Strait of Juan de Fuca, Puget Sound, Olympic peninsula and Sequim Bay area. The second region is set for specific area around the CSZ source region. The third region are set for strait of Juan de Fuca. The forth to sixth region are set in different resoluiton for the final goal of 1/3 sec simulation around Sequim Bay. Table 1 shows the longitude, latitude and resolution of each region. The elapsed simulation time is 10 hours, starting at the time of the earthquake. The boundary condition method is extrapolation, that lets wave pass out of the boundary without reflection. Resolution varies for each domain with adaptive mesh refinement. The coarsest resolution, 12 arc minutes, is set for tsunami propagation in the large domain. The finest resolution 1/3 arc second is set to calculate inundation in Sequim bay area. Two-hundred numerical gauges are set around Sequim Bay (Figure 4) to record simulated wave height and water speed at those points in the model.

Table 1: The nested computational domains for use in Geoclaw.

Region	Longitude(W)	Latitude(S)	Resolution (degrees)
1	-129 to -122	45 to 52	12 min
2	-127 to -123	45 to 49	1 min
3	-125.120046 to -122.20046	47.909954 to 48.789954	1 min
4	-123.18 to -122.2	47.02 to 47.909954	10 sec
5	-123.065269 to -122.977493	48.011011 to 48.087751	2 sec
6	-123.05106482 to -122.98893519	48.01716667 to 48.085046296	1/3 sec

3.4 The rupture scenario

The seafloor displacement for this study is based on one of the fifteen earthquake source scenarios in Witter et al. (2011). In the model, Geoclaw uses rupture geometry to determine the initial sea surface elevation based on the half-space elastic fault plane model by Okada (1985). The Okada model assumes the initial sea surface elevation exactly follow the vertical motion of the seafloor displacement, because the water column over the rupture zone is unable to drain out instantaneously. The full-margin rupture scenario with slip partitioned to a splay fault is modeled with vary slip distribution base on turbidite paleoseismic records and constraints from the tsunami simulation at Bradley Lake (Goldfinger et al., 2012, Witter et al., 2011). The large splay fault model (L1) is selected in this study because the scenario is thought to represent roughly a 2500-year event encompassing ~80 to 95 percent of the hazard. The source parameters are listed in Table 2.

Table 2: The L1 source parameters.

Rupture scenario	L1
Length (km)	1,000
Width (km)	83
Maximum slip (m)	27
Average Slip (m)	13
Interevent time (yrs)	2500

4.0 Results:

4.1 Initial sea surface elevation

Figure 5a shows the modeled coseismic uplift (red) and subsidence (blue) for the L1 scenario at 0.1 second after the earthquake. Figure 5b displays an enlarged region for the coast of Washington. The maximum sea surface elevation change due to the modeled earthquake is about 13 meters outside the Strait of Juan de Fuca.

4.2 Tsunami propagation

A sequence of snapshots of tsunami wave propagation every hour is presented in Figure 6. The tsunami generated by the L1 scenario would impact most severely the coast of the Pacific Ocean, Strait of Juan de Fuca and Puget Sound. The tsunami energy starts to decrease 5 hours after the earthquake.

The sequence of snapshots of tsunami wave propagation in Sequim bay are presented in Figure 7. The water starts to withdraw from the bay at about 60 minutes after the earthquake happens. Then, the first wave arrives 45 minutes later. The first arrival wave has a maximum wave height around 2 meters at 120 minutes after the earthquake. Then, the waves remain in the bay. The second wave arrives at the bay at about 240 minutes after the earthquake. The third and fourth waves arrive in the bay at 360 minutes and 480 minutes after the earthquake, and have smaller aptitude compared with the first two waves.

The sequence of snapshots of tsunami wave propagation in Bell Creek Valley near the entrance of Sequim Bay are presented in Figure 8. The first wave arrives the valley at 105 minutes after the earthquake in the valley and floods the entire lagoon. The wave inundates inland about 1 kilometer. The second wave arrives the valley at 225 minutes after the earthquake.

4.3 Maximum flooding depth

Figure 9 shows the maximum flooding depth of L1 scenario sweeps across the bay. The flood depth is about 4-5 meters height near the entrance of the bay. Travis Spit is overtopped by 2-3

m at maximum flood depth. The marine laboratory at the entrance to Sequim Bay is inundated. Pitship Point (the location of a marina), Pitship pocket estuary, Schoolhouse Point, Hardwick Point, and Paradise Cove are all over-topped. The maximum flood depth is about 2-3 meter in the bottom of the bay, with as much as 2 m inundation in the shoreline areas of Blyn.

Figure 10 shows the maximum flooding depth in the Bell Creek Valley. The maximum flood depth is about 5.0 meters at the west edge of The Lagoon. Gibson Spit is over-topped by 3-4 m. Washington Harbor road, a local farm, and a municipal sewage treatment plant are within or close to the inundation zone.

4.4 Maximum speed

Figure 11 shows the maximum speed in Sequim Bay. Vortices can be found in the bay, caused by the local topography. The spit which almost encloses Sequim Bay creates a narrow passage to allow the tsunami waves into the bay. The velocity of the tsunami waves increases after passing through the narrow passage and shallow shelf at the entrance to the bay.

4.5 Numerical gauges

Two hundred numerical gauges were set along the coast of the bay and in the bay to provide detailed information about wave height and arrival times. Figure 12(a) shows a numerical gauge in The Lagoon area. The wave height is about 4 meters height in this area. Figure 12(b) displays a numerical gauge near the entrance of the bay, while figure 12(c) displays a numerical gauge near the southern end of the bay. Four waves appear in 10 hours, so the tsunami period is about 2.5 hour. The first arrival wave is around 2 meters after a -0.8 meters negative wave. The second arrival wave shows similar wave height with the first arrival wave. However, the second wave is slightly smaller than the first wave in Figure 12(b), while the second wave is slightly larger than the first wave in Figure 12(c). The third arrival wave start to decrease. Figure 12(d) shows a numerical gauge in the middle of the bay. The wave form has less high-frequency signal compare to other gauges due to the deeper water.

4.6 Tsunami arrival time

Figure 13 shows the arrival time after the earthquake of the first tsunami wave in Sequim Bay. In the whole Sequim bay, tsunami waves arrive about 90 to 100 minutes after the earthquake. Some areas in the bottom of the bay will be inundated in 120 minutes, which is between the first wave and the second wave. Figure 14 shows the time of the maximum wave in the Sequim bay. The first tsunami wave causes higher maximum wave height than the second tsunami wave in the northern part of the bay, while the second tsunami wave cause higher maximum wave than the first tsunami wave in the southern part of the bay. Figure 15 shows the first tsunami arrival time in Bell Creek Valley. Tsunami waves arrive about 80 to 100 minutes after the earthquake.

4.7 Inundation on land with GIS analysis

Figure 16a shows the tsunami inundation overlap with a property map for Sequim Bay. The inundation to private property happens only in the southern end of the bay and the entrance of Bell Creek valley. In the entrance of Bell Creek Valley, the inundation is about 1-5 meters depth (Figure 16b). The inundation zone with the distant flood inland in the valley is about 300 meters. At the southern end of the bay, the inundation is 1-2 meters depth (Figure 16c). Private property damage, estimated by value of the buildings, is about $700,000 in the inundation zone in Sequim Bay area. This does not include potential damage to the marine science lab or loss of business revenue in Blyn, the marina, or other tourist facilities or private shoreline improvements around the bay.

The enclosed geomorphic features in Sequim Bay cause different tsunami behaviors compared with nearby Discovery Bay. The tsunami waves in Sequim Bay have smaller wave height but remain longer in the bay than the tsunami waves in the Discovery Bay (Figure 17).

5.0 Discussion:

A tsunami generated at the Cascadia Subduction Zone would impact severely along the coast of Washington State. My simulation results show that the tsunami waves generated by CSZ will

enter the Strait of Juan de Fuca and impact Puget Sound, and in particular, Sequim Bay. The snapshots of wave propagation and numerical tidal gauges indicate at least four major waves will enter the bay over ten hours simulation. The first wave and second wave have similar wave amplitude. The reason for the similar wave amplitude might be the geomorphic features around which the initial wave reflects and refracts within Strait and Puget Sound. Also, the Strait of Juan de Fuca behaves as a narrow passage to concentrate the tsunami waves.

My particular interest is the tsunami effects in Sequim Bay. The wave propagation and wave height are strongly affected by the spit and bathymetry in Sequim Bay. The spit in the entrance of the bay creates an almost enclosed system for Sequim Bay. Also, the bathymetry in the western bay has more gentle change in elevation than in the eastern bay. The maximum wave height plot (Figure 9) shows that Travis spit plays an important role for protecting the bay from tsunami attacks. Although the Travis spit is overtopped during the first and second tsunami waves, higher amplitude of the wave is calculated offshore from the spit than inside the bay (Figure 7). The maximum wave height inside the spit area is about 2 meters height, while the maximum wave height outside the spit area is about 3 meters height. The arrival time of first arrival tsunami waves are also different inside and outside the spit. The first wave arrives in the valley outside the split about 80 to 90 minutes after the earthquake, while the maximum wave arrives inside the bay about 90 to 120 minutes after the earthquake (Figure 13). The spit has diminished and delayed the tsunami impacts in Sequim Bay.

The simulation result of the maximum speed plot shows a high speed pattern along the western coast of Sequim Bay (Figure 11), that has the potential to increase erosion along the shoreline of the bay. This erosion is not simulated by the model. Sediment transport models could be useful for tackling this problem in future work. The high velocity of tsunami waves might be caused by bathymetry. When the tsunami moves through the narrow entrance to the bay, the wave velocity is increased. Also, the shallow bathymetry at the upper western bay might trap the energy. The tsunami wave might turn into edge waves when it propagates across the shallow bathymetry. However, edge wave induced by tsunamis have not been observed in

Sequim Bay. More details have to be done in future work to determine the possible edge wave effects.

Inundation happens in the entrance of the Bell Creek Valley and the southern end of Sequim Bay. The distance of tsunami flood inland in the entrance of the valley is about 300 meters. The depth of inundation is about 1-5 meters depth. The local bathymetry and vegetation impact the inundation in this area. I use the Manning's *n* of 0.025 to assume the terrain in the model is very smooth, providing a conservative estimate of inundation. In other words, the valley concentrates the tsunami waves, also the smooth terrain allows the tsunami to run farther inland.

At the southern end of the bay, the inundation is 1-2 meters depth. Although a wave of 1-2 meters height seems not that high, the destruction of the wave is unneglectable. The long-wavelength tsunami waves could cause more damage than the short-wavelength wind wave. The tsunami wave will remain in the bay for a long time. Also, Highway 101, an important evacuation route, is located nearby this tsunami inundation zone, suggesting that alternate evacuation routes may be required.

The modeled inundation area helps identify regions to search for tsunami deposits. The tidal marshes that had been inundated might have a chance to preserve the tsunami deposits. Tsunami inundation areas include part of the Marine laboratory, the Marina, Pitship pocket estuary, School house point, Paradise Cove, Hardwick point and part of tidal marsh near Blyn. Considering that some of these locations have been disturbed by construction or human activities, future tsunami deposit investigations may want to look in The Lagoon, Paradise Cove, and Pitship Pocket Estuary.

6.0 Conclusions:

This study modeled tsunami propagation and inundation along the Sequim Bay based on a Mw 9.0 CSZ earthquake. I adopted a tsunami model, Geoclaw, with 10-meters resolution to conduct

the simulation. Modeling result shows that about 4-5 meters height wave amplitude is in the entrance to Bell Creek Valley, and about 2-3 meters height wave amplitude is in the bay. Also, the results show the inundation happens in the entrance of the valley and the southern end of the bay and some spots along the shoreline. The inundation is 1-2 meters depth at the southern end of the bay, while the inundation is about 1-5 meters depth in the entrance of the valley. The enclosed system of Sequim bay and bathymetry have significant impact on tsunami dynamics. The arrival time of maximum wave in the bottom of the bay (120 minutes) is about 15 minutes later than the arrival time in the entrance of the valley (105 minutes). The spit makes the tsunami waves in Sequim bay have smaller wave height but remain longer time than the tsunami waves in Discovery Bay. I estimate roughly $700,000 in properties are located in the inundation zone. Also, the business revenue around the bay is estimated to be over $3.8 million. It is my hope that these modeling results will be useful for public safety administration in the Pacific Northwest as an aid to development of hazard mitigation plans and emergency response, also, potentially, to further paleotsunami research, by identifying possible past inundation areas.

7.0 References:

1. Amante, C. and Eakins, B. W., 2009, ETOPO1 1 Arc-Minute Global Relief Model: Procedures, Data Sources and Analysis. *NOAA Technical Memorandum NESDIS NGDC-24*, 19 pp
2. Arcos, M. E. M., and LeVeque R. J., 2015, Validating velocities in the GeoClaw tsunami model using observations near Hawaii from the 2011 Tohoku tsunami: Pure and Applied Geophysics, vol. 172, issue 3-4, p.849-867.
3. Atwater, B., 1987, Evidence for great Holocene earthquake along the Outer coast of Washington State: Secience, vol. 236, no. 4804, p.942-944.
4. Atwater, B.F., Musumi-Rokkaku, S., Satake, K., Tsuji, Y., Ueda, K., and Yamaguchi, D.K., 2015, The orphan tsunami of 1700—Japanese clues to a parent earthquake in North America, 2nd ed.: Seattle, University of Washington Press, U.S. Geological Survey Professional Paper 1707, 135 p.
5. Borerro, J. C., LeVeque, R. J. Greer, S. D., O'Neill, S., and Davis B. N., 2015, Observation and modelling of tsunami currents at the Port of Tauranga, New Zealand: Australasian Coasts & Australasian Coasts & Ports Conference.
6. Carignan, K.S., McLean S. J., Eakins B. W., Beasley L., Love M.R., and Sutherland M., 2014, Digital Elevation Model of Puget Sound Washington: Procedures, Data Source, and Analysis, NOAA National Geophysical Data Center (assessed August 2016).
7. Clawpack Development Team, 2017, Clawpack software version 5.4.0 http://www/clawpack.org, doi:10.5281/zenodo.262111.
8. Dean, R. G. and Dalrymple, R. A., 1991, Water Wave Mechanics for Engineers and Scientists: World scientific pub. Co., Teaneck, NJ.
9. Elwha-Dungeness Planning Unit, 2005, Elwha-Dungeness Watershed Plan, Water Resource Inventory Area (WRIA 18) and Sequim Bay in West WRIA 17. Volume 1: Chapters 1-3 and 15 appendices; Volume 2: Appendix 3-E. http://www.clallam.net/environment/assets/applets/W18_TitlePageVol1.pdf (accessed June 2016)

10. Geist, E. L., 2005, Local tsunami hazards in the Pacific Northwest from Cascadia Subduction Zone Earthquake: U. S. Geological Survey Professional Paper 1661B.
11. Goldfinger, C., 1994, Active deformation of the Cascadia forearc: implications for great earthquake potential in Oregon and Washington (PhD dissertation thesis): Corvallis, Oregon, Oregon State University, 202 p.
12. Goldfinger, C., Nelson, C.H., Morey, A., Johnson, J.E., Gutierrez-Pastor, J., Eriksson, A. T., Karabanov, E., Patton, J., Gracia, E., Enkin, R., Dallimorem A., Dunhill, G., and Vallier, T., 2012, Turbidite event history: Methods and implications for Holocene Paleoseismicity of the Cascadia Subduction Zone: U.S. Geological Survey Professional Paper 1661-F, 178 p.
13. Gonzalez, F. I., LeVeque, R. J., Varkovitzky J., Chamberlain P., Hirai B., and George D. L., 2011, Validation of the GeoClaw model: NTHMP MMS tsunami inundation model validation workshop. http://depts.washington.edu/clawpack/links/nthmp-benchmarks/geoclaw-results.pdf
14. Gonzalez, F. I., LeVeque, R. J., Loyce, M. A., 2013a, Tsunami Hazard Assessment of the Elementary School Berm Site in Long Beach, WA: UW libraries research works digital repository: http://hdl.handle.net/1773/22705
15. Gonzalez, F. I., LeVeque, R. J., Loyce, M. A., 2013b, Probabilistic Tsunami Hazard Assessment (PTHA) for Crescent City, CA. Final Report for Phase I: UW libraries research works digital repository: http://hdl.handle.net/1773/22366.
16. Google Inc., 2016, Google Earth Pro version 7.1.7.2606 https://www.google.com/earth/download/gep/agree.html
17. Hayes G.P., and Furlong K. P., 2010, Quantifying potential tsunami hazard in the Puysegur subduction zone, south of New Zealand: Geophysical Journal International, p.1512-1524.
18. Heaton, T. H. and Hartzell S. H., 1987, Earthquake hazards on the Cascadia subduction zone, Science 236.
19. Hopper, M. G., Langer, C. J., Spence, W. J., Rogers, A. M., Algermissen, S. T., 1975, A study of earthquake losses in the Puget Sound, Washington, area: U. S. Geological Survey Open-File Report75-375, 298p.

20. Kilfeather, A. A., Blackford, J. J., and Van Der Meer, J. J. M., 2007, Mocromorphological analysis of coastal sediments from Willapa Bay, Washington, USA: a technique for analysising inferred tsunami deposits: Pure Appl. Geophys. 164, 509-525.
21. Kirby, J. T., Wei, G., Chen, Q., Kennedy, A. B. and Dalrymple, R. A., 1998, FUNWAVE 1.0, fully nonlinear Boussinesq wave model. Documentation and user manual: Report CACR-98-06, Center for Applied Coastal Research, University of Delaware.
22. LeVeque, R., George, D., & Berger, M., 2011, Tsunami modelling with adaptively refined finite volume methods: *Acta Numerica, 20*, 211-289. doi:10.1017/S0962492911000043
23. Liu, P. L.-F., Woo, S.-B. and Cho, Y.-S., 1998, Computer program for tsunami propagation and inundation, Tech. rep., Cornell University.
24. Liu, P. L.-F., Yeh, H., Synolakis, C., 2008, Advanced numerical models for simulating tsunami waves and runup: world scientific publishing company, Singapore.
25. Lynett, P., Wu, T. -R. and Liu P. L.-F., 2002, Modeling wave runup with depth-integrated equations: Coastal Engineering, vol. 46, issue 2, p.89-107.
26. Mader, C. L., 1988, Numerical modeling of water waves: University of California Press, Berleley.
27. McCrory, P.A., Blair, J.L., Oppenheimer, D.H., and Walter, S.R., 2004, Depth to the Juan de Fuca slab beneath the Cascadia Subduction Margin—a 3-D model for sorting earthquakes: U.S. Geological Survey Data Series DS-91, 13 p.
28. Morey, A. E., Goldfinger, C., Briles C. E., Gavin D. G., Colombaroli, D., and Kusler J. E., 2013, Are great Cascadia earthquakes recorded in the sedimentary records from small forearc lakes?: Nat. Hazards Earth Syst. Sci., 13, p. 2441-2463.
29. Murata, S., Imamura, F., Katoh, K., Kawata, Y., Takahashi, S., and Takayama, T., 2010, To survive from tsunami: Advance series on ocean engineering 32.
30. Okada, Y., 1985, Surface deformation due to shear and tensile faults in a half-space: Bulletin of the Seismological Society of America, v. 75, no. 4, p.1135-1154.
31. Petersen, M.D., Cramer, C. H., and Frankel, A. D., 2002, Simulations of seismic hazard for the Pacific Northwest of the United States from earthquakes associated with the Cascadia subduction zone: Pure Appl. Geophys., vol. 159, p.2147–2168.

32. Puget Sound River History Project, University of Washington. http://riverhistory.ess.washington.edu
33. Satake, K., Shimazaki, K., Tsuji, Y., and Ueda, K., 1996, Time and size of a giant earthquake in Cascadia inferred from Japanese tsunami records of January 1700: Nature 379, p.246-246.
34. Schasse, H.W., 2003, Geologic Map of Washington portion of the Port Angeles 1:100,000 quadrangle: Washington Division of Geology and Earth Resources Open File Report, scale 1:100,000.
35. Titov, V. V. and Gonzalez F. I., 1997, Implementation and testing of the Method of Splitting Tsunami (MOST) model: NOAA Technical Memorandum ERL PMEL-112.
36. Todd, S., Fitzpatrick, N., Carter-Mortimer, A., and Weller C., 2006, Historical changes to estuaries, spits, and associated tidal wetland habitats in the Hood canal and strait of Juan de Fuca regions of Washington State, Appendix B-4: Sequim Bay sub-region: PNPTC technical report.
37. Walsh, T. J., Myers, E. P., and Baptista, A. M., 2002a, Tsunami inundation map of the Port Angeles, Washington area: Washington Division of Geology and Earth Resources Open File Report 2002-1, 1 sheet, scale 1:24,000.
38. Walsh, T. J., Myers, E. P., and Baptista, A. M., 2002b, Tsunami inundation map of the Port Townsend, Washington area: Washington Division of Geology and Earth Resources Open File Report 2002-2, 1 sheet, scale 1:24,000.
39. Witter R. C., Zhang Yinglong, Wang Kelin, Priest G. R., Goldfinger C., Stimely L. L., English J.T., Ferro, P. A., 2011, Simulating tsunami inundaion at Bandon, Coos County, Oregon, using hypothetical Cascadia and Alaska earthquake scenarios. Oregon Department of Geology and Mineral Industries Special Paper, p. 43-57.
40. Williams H. F.L., Hutchinson I., Nelson A. R., 2005, Multiple sources for late-Holocene tsunamis at Discovery Bay, Washington State, USA: The Holocene, vol. 15, no. 1, p. 60-73.

41. Wood N. and Soulard C., 2008, Variations in Community Exposure and Sensitivity to Tsunami Hazards on the Open-Ocean and Strait of Juan de Fuca Coasts of Washington: USGS Scientific Investigation Report.
42. Yu, F.J., Wang P.T., Zhao, L. D., and Yuan Y., 2011, Numerical simulation of the 2010 Chile tsunami and its impact on Chinese coast: Chinese Journal of Geophysics, pp. 918-928 (in Chinese).
43. Zhang, S., Yuen D. A., Zhu A., and Song, S., 2011, Use of many-core Architectures for high-resolution Simulation of Tohoku 2011 tsunami waves: SC-11 International Conference for High Performance Computing.

8.0 Figures:

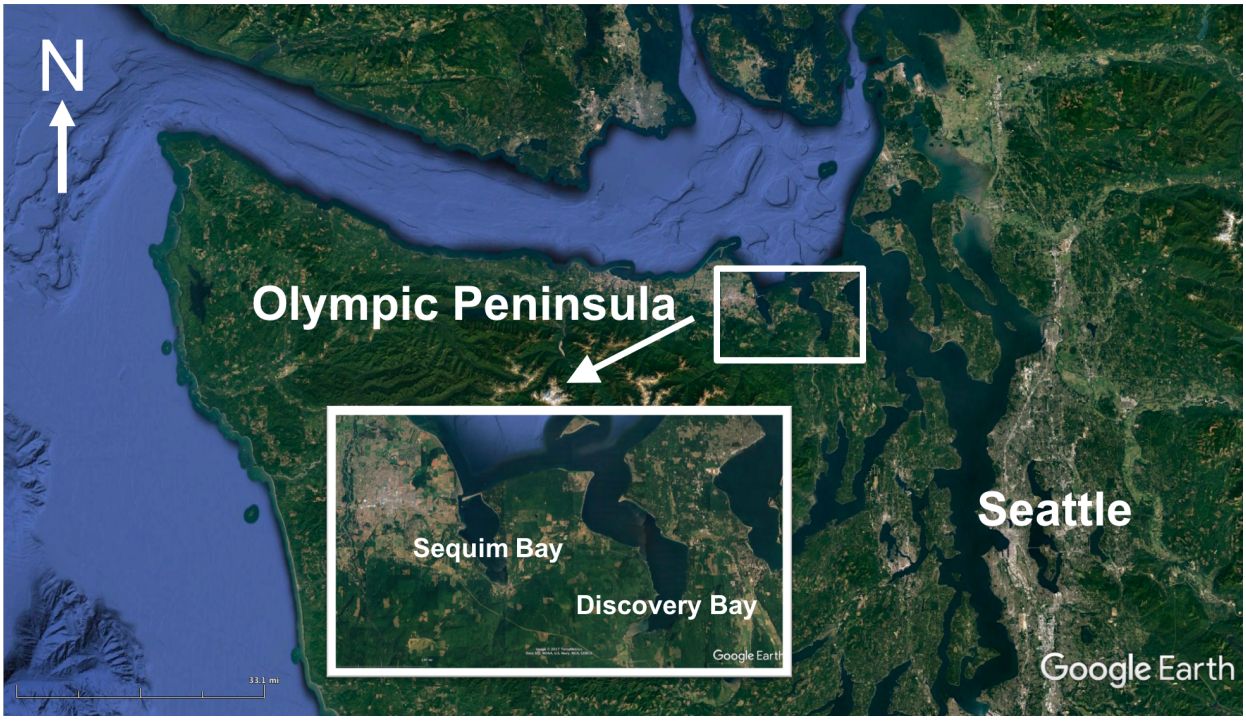

Figure 1： Location of Sequim Bay and Discovery Bay on the Olympic Peninsula, Washington (Google Earth Pro, 2016).

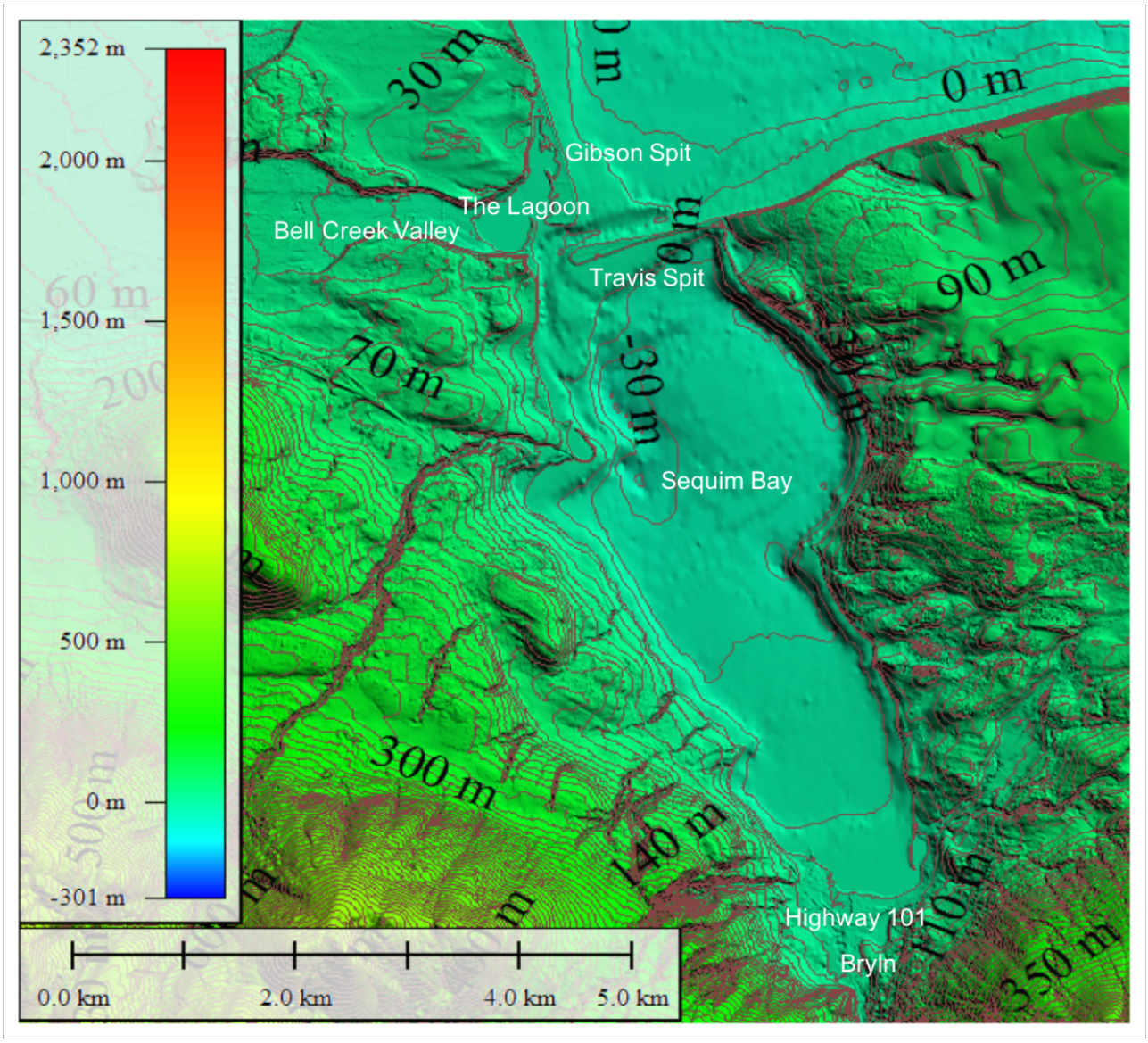

Figure 2：Bathymetry and topography at Sequim Bay. (Global Mapper, 2016)

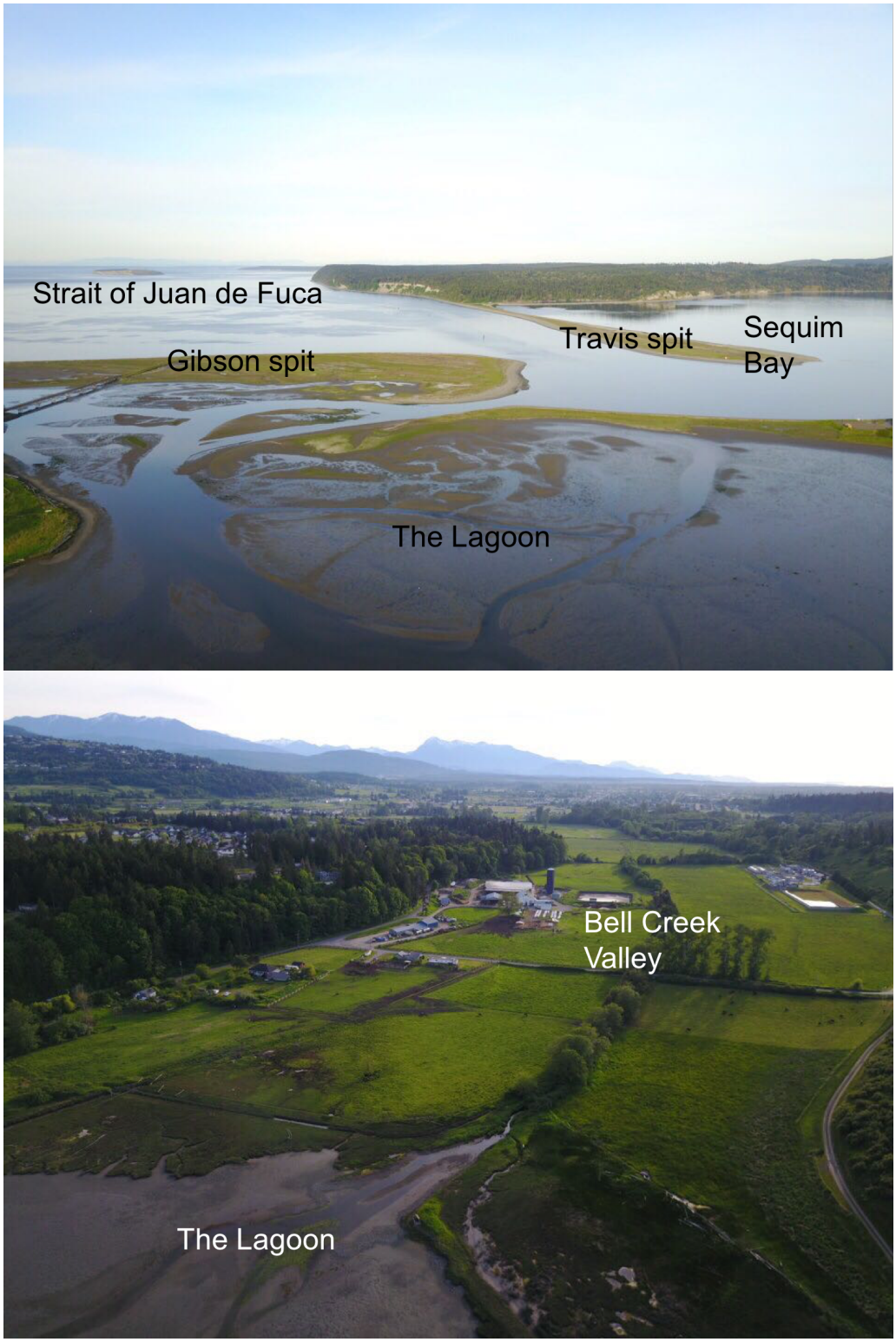

Figure 3：Oblique aerial photos of Gibson and Travis spits, The Lagoon and Bell Creek Valley.

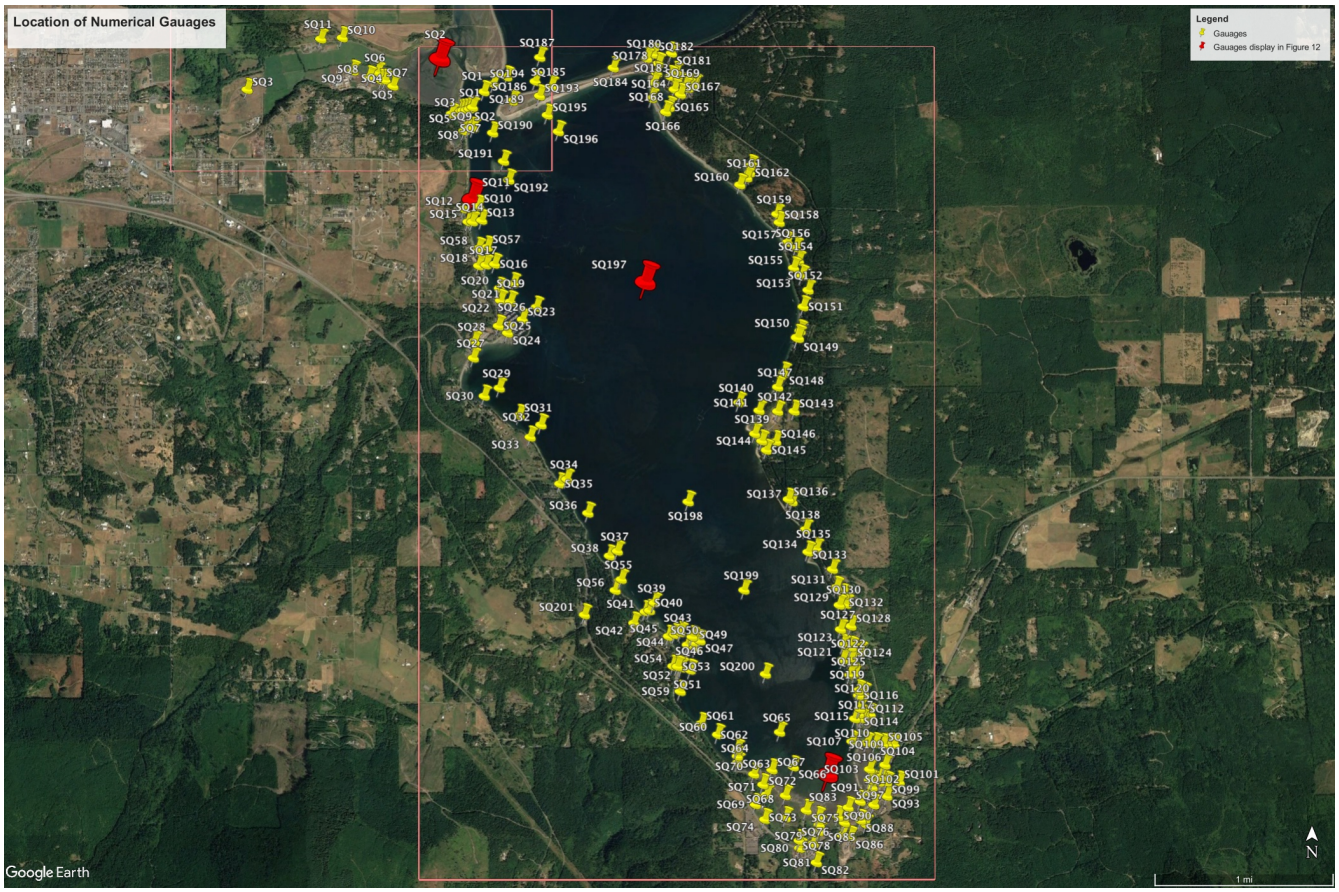

Figure 4：Location of numerical gauges placed in the model of Sequim Bay to record wave height and water velocity. Red box shows limits of high-resolution model domain. The red marks indicate the location of gauges displaed in Figure 12. (Base image from Google Earth Pro, 2016.)

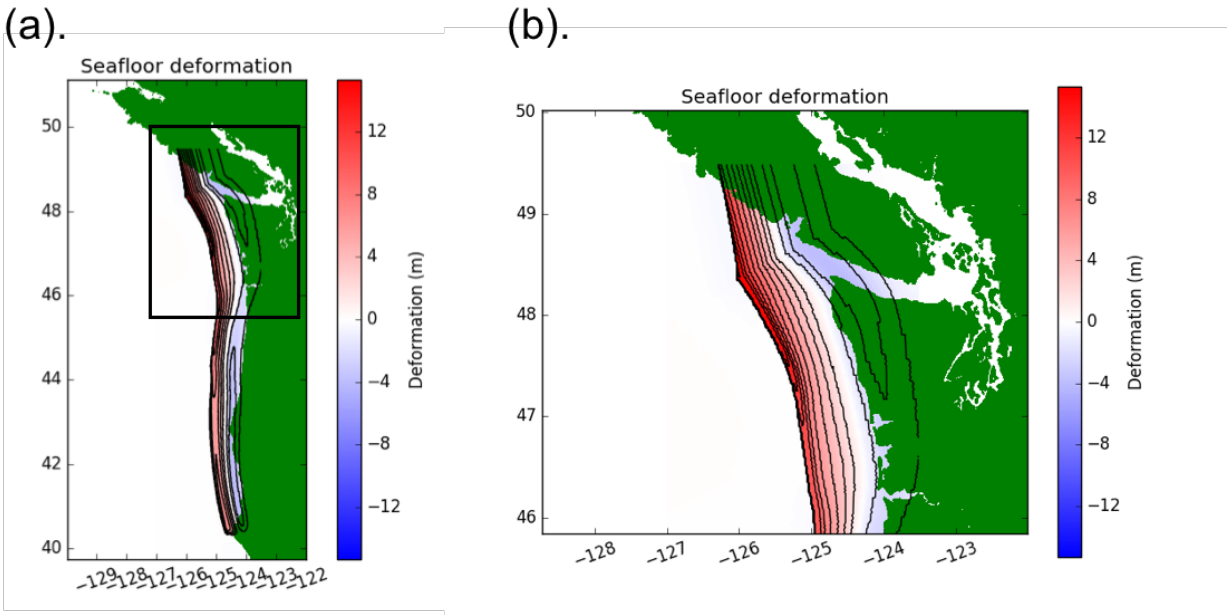

Figure 5： (a) The initial free surface elevation of the wave. (b) Enlarged view to show the initial free surface elevation around the coast of Washington and entrance to the Strait of Juan de Fuca. Red represents uplift. Blue represents subsidence.

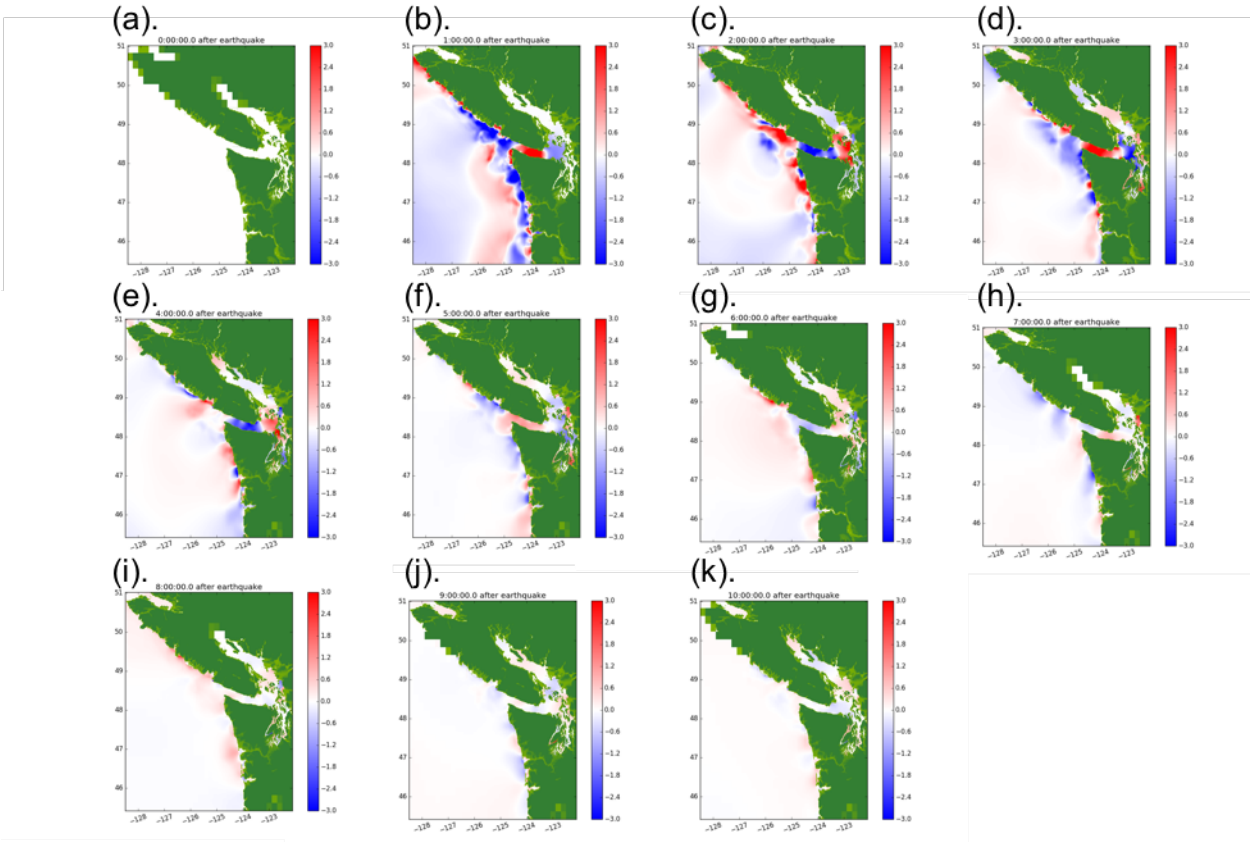

Figure 6：Sequence of snapshots of water elevation for the earthquake-induced tsunami scenario at the Juan de Fuca strait. Color scale shows water height relative to mean high water, with deepest red at +3 m, and darkest blue at -3 m. (Tidal effects are not included.) (a) t= 0 s, (b) t= 1 hour, (c) t= 2 hours, (d) t= 3 hours, (e) t= 4 hours, (f) t= 5 hours, (g) t= 6 hours, (h) t= 7 hours, (i) t= 8 hours, (j) t= 9 hours, (k) t= 10 hours

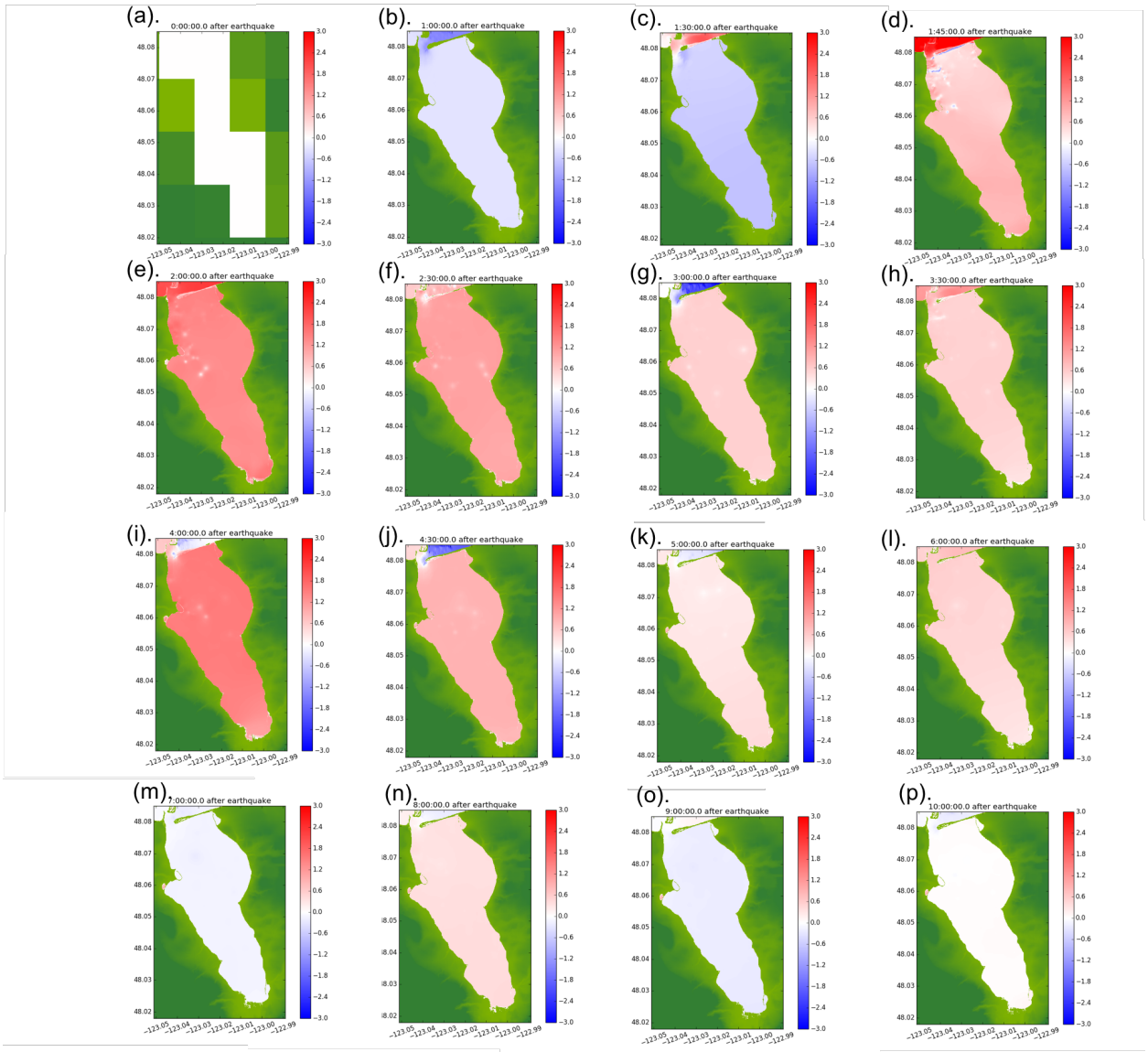

Figure 7：Sequence of snapshots of water elevation for the earthquake-induced tsunami scenario at the Sequim Bay. Color bar as in Fig. 6.(a) t= 0 s, (b) t= 60 minutes, (c) t= 90 minutes, (d) t= 105 minutes, (e) t= 120 minutes, (f) t= 150 minutes, (g) t= 180 minutes, (h) t= 210 minutes, (i) t= 240 minutes, (j) t= 270 minutes, (k) t= 300 minutes, (l) t= 360 minutes, (m) t= 420 minutes, (n) t=480 minutes, (o) t=540 minutes, (p) t=600 minutes

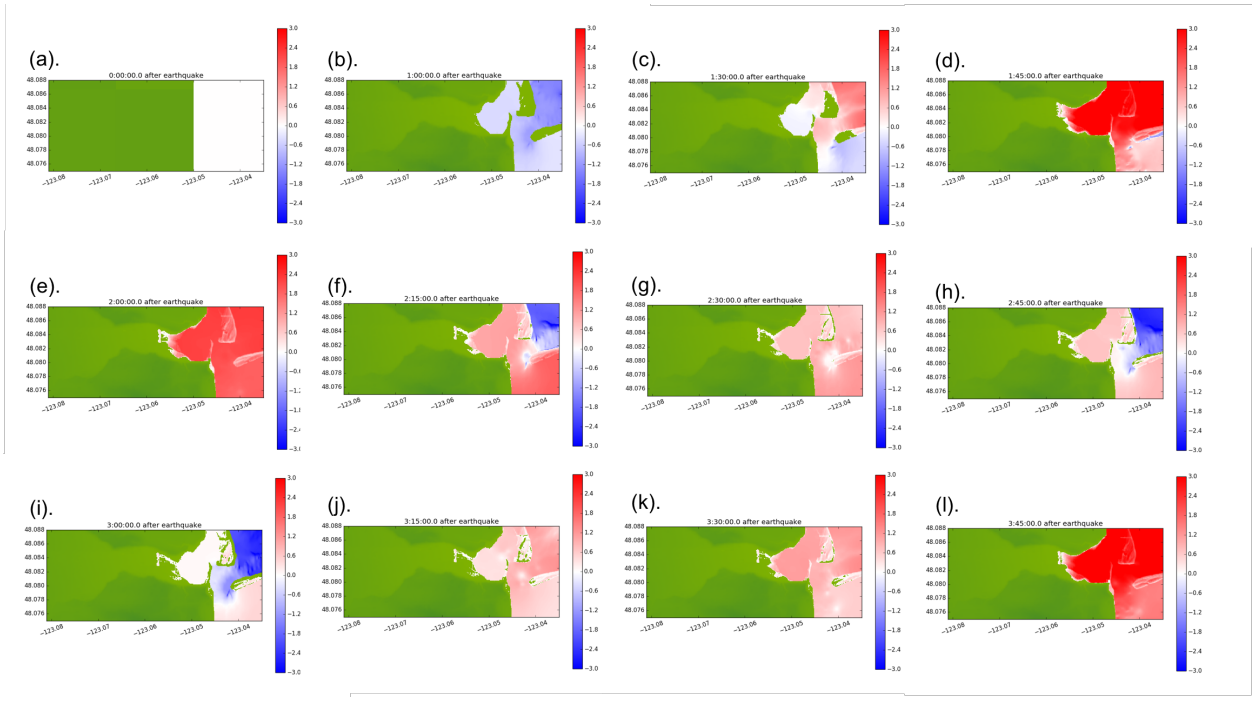

Figure 8：Sequence of snapshots of water elevation for the earthquake-induced tsunami scenario at the entrance of the valley. Color bar as in Fig. 6. (a) t= 0 minutes, (b) t= 60 minutes, (c) t= 90 minutes, (d) t= 105 minutes, (e) t= 120 minutes, (f) t= 135 minutes, (g) t= 150 minutes, (h) t= 165 minutes, (i) t= 180 minutes, (j) t= 195 minutes, (k) t= 210 minutes, (l) t= 225 minutes

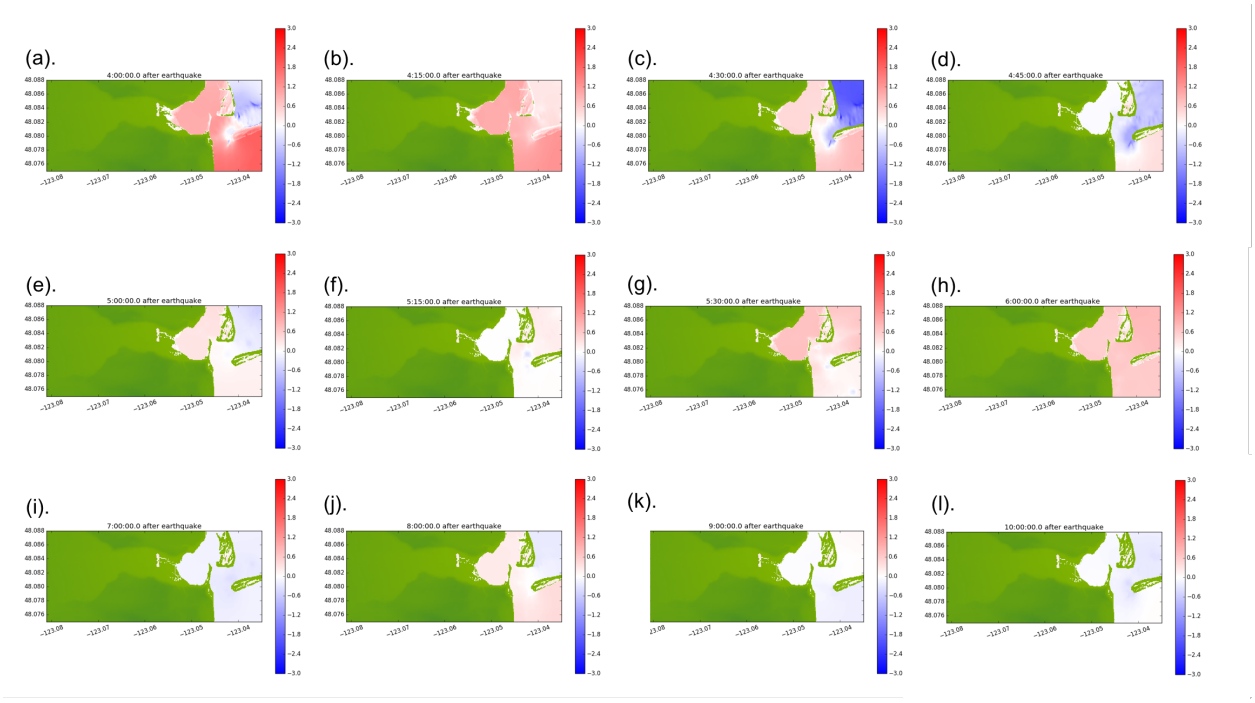

Figure 8 (continued): Sequence of snapshots of water elevation for the earthquake-induced tsunami scenario at the entrance of the valley. (a) t= 240 minutes, (b) t= 255 minutes, (c) t= 270 minutes, (d) t= 285 minutes, (e) t= 300 minutes, (f) t= 315 minutes, (g) t= 330 minutes, (h) t= 360 minutes, (i) t= 420 minutes, (j) t= 480 minutes, (k) t= 540 minutes, (l) t= 600 minutes

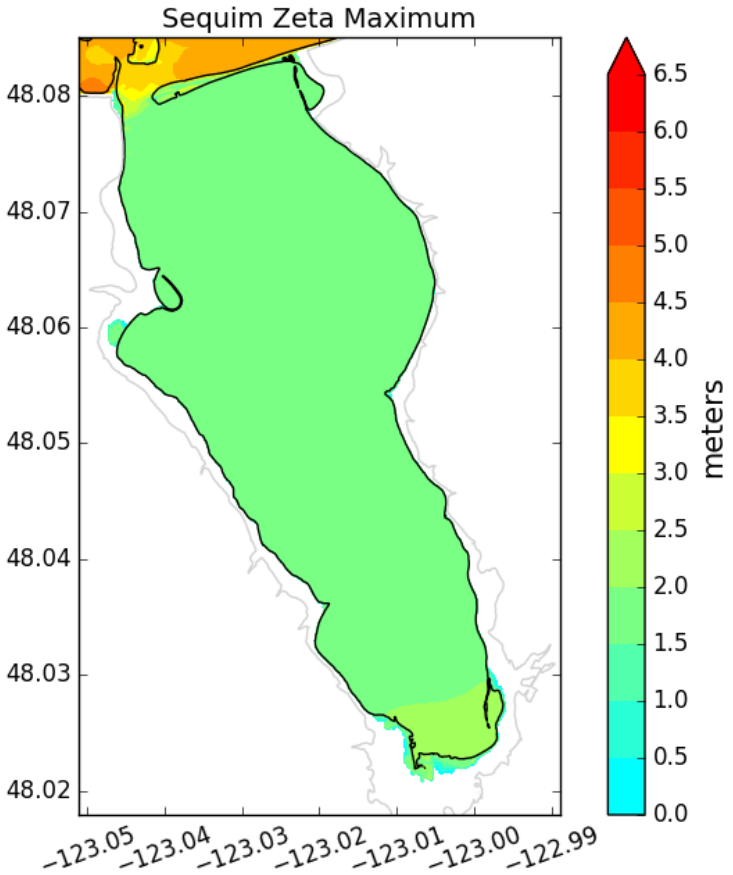

Figure 9：Maximum flooding depth for L1 scenario in Sequim Bay. The light grey line indicates the 20 meter elevation contour.

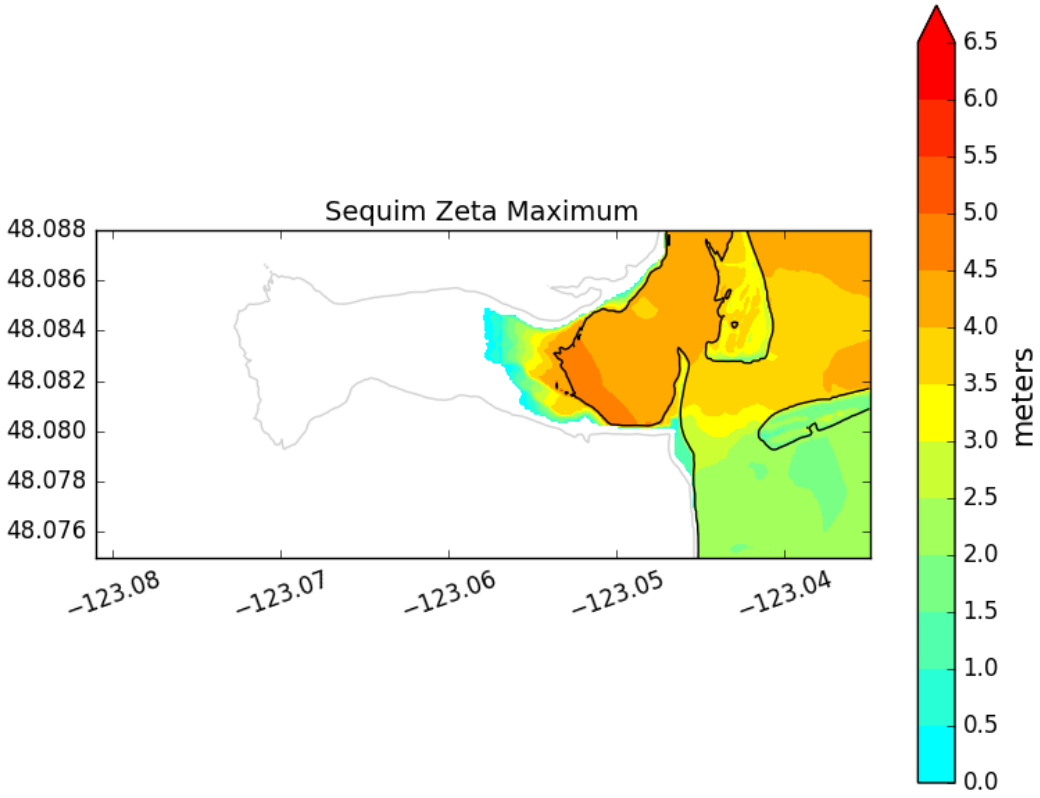

Figure 10：Maximum flooding depth for L1 scenario in the Bell Creek Valley. The light grey line indicates the 20 meter elevation contour.

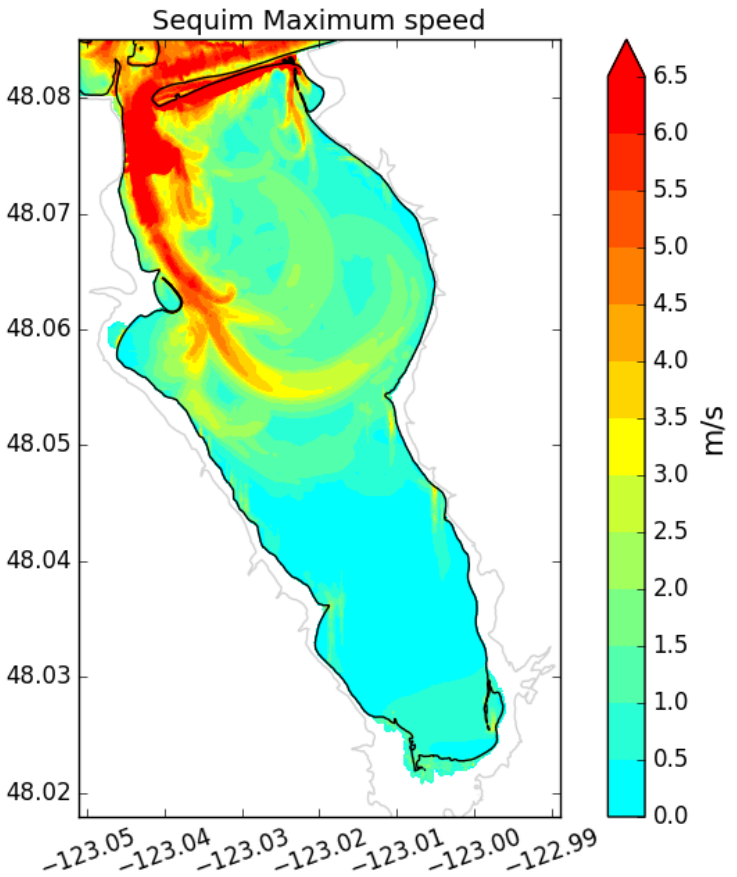

Figure 11：The maximum tsunami wave speed in Sequim Bay. The light gray line indicate the 20 meter elevation contour.

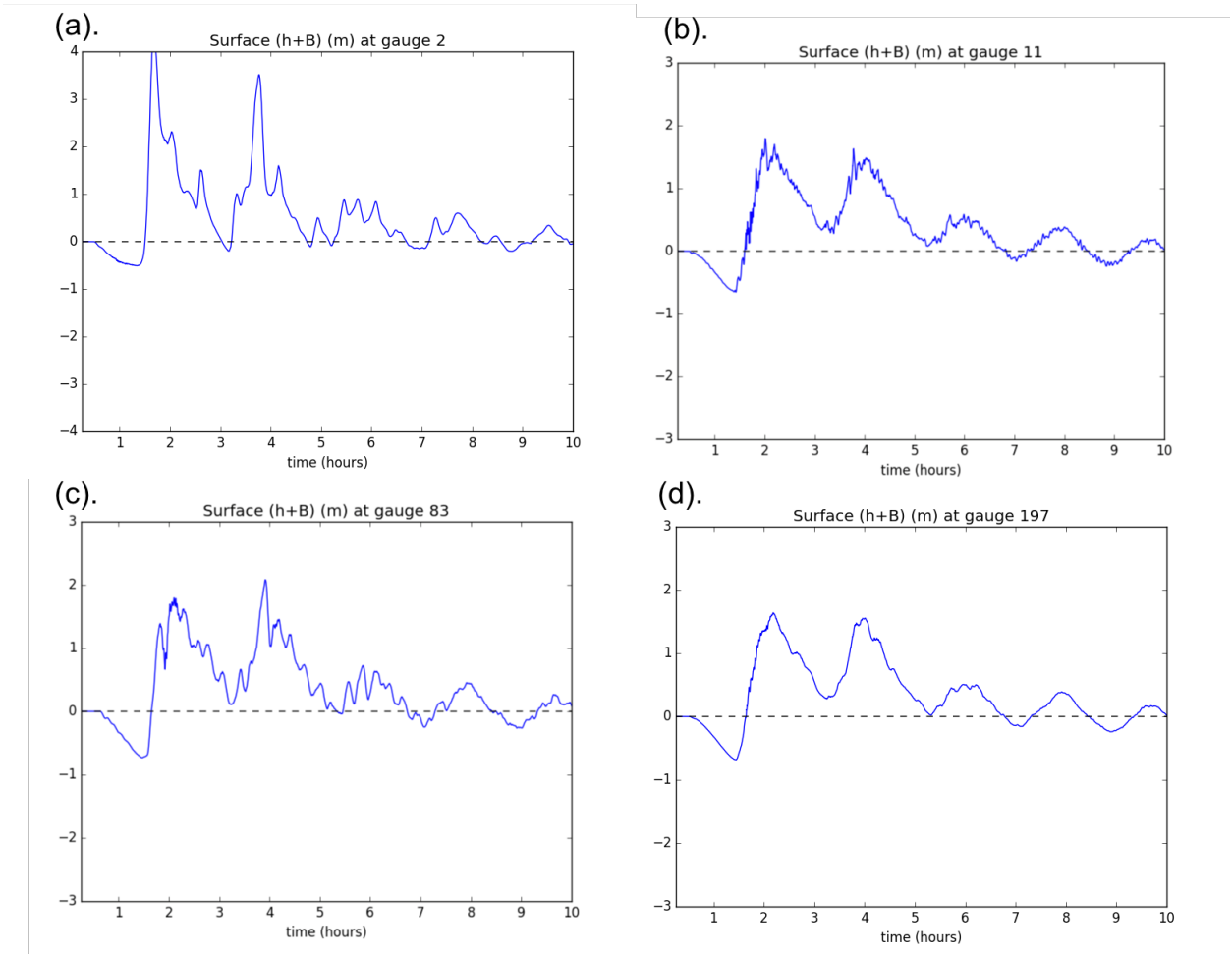

Figure 12： (a) Numerical gauage in The Lagoon. (b) Numerical gauage near the entrance of the bay. (c) Numerical gauge near the bottom of the bay. (d) Numerical gauage in the middle of the bay. The value displayed is the sea-surface elevation, which is a sum of water depth and bathymetry.

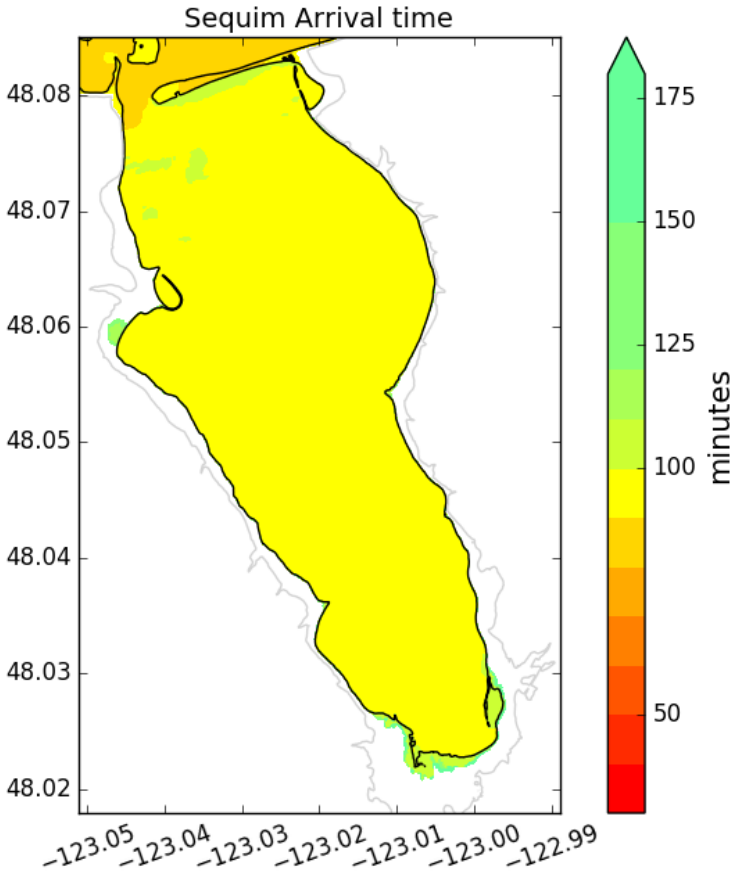

Figure 13：Arrival time of first tsunami wave along Sequim Bay (minutes after the earthquake).

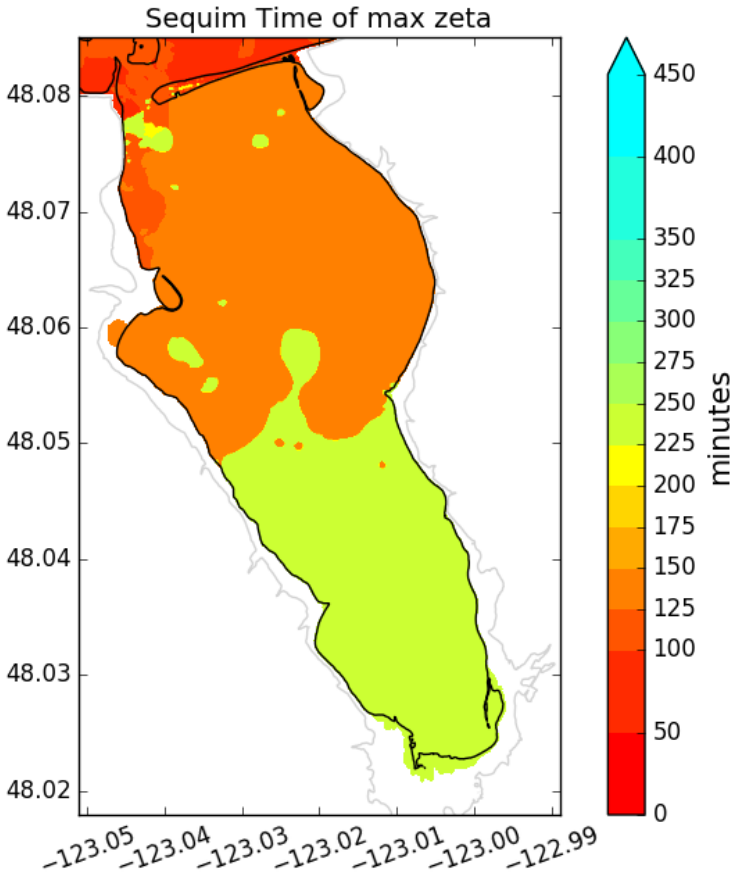

Figure 14：Time of the maximum wave in Sequim Bay (minutes after the earthquake).

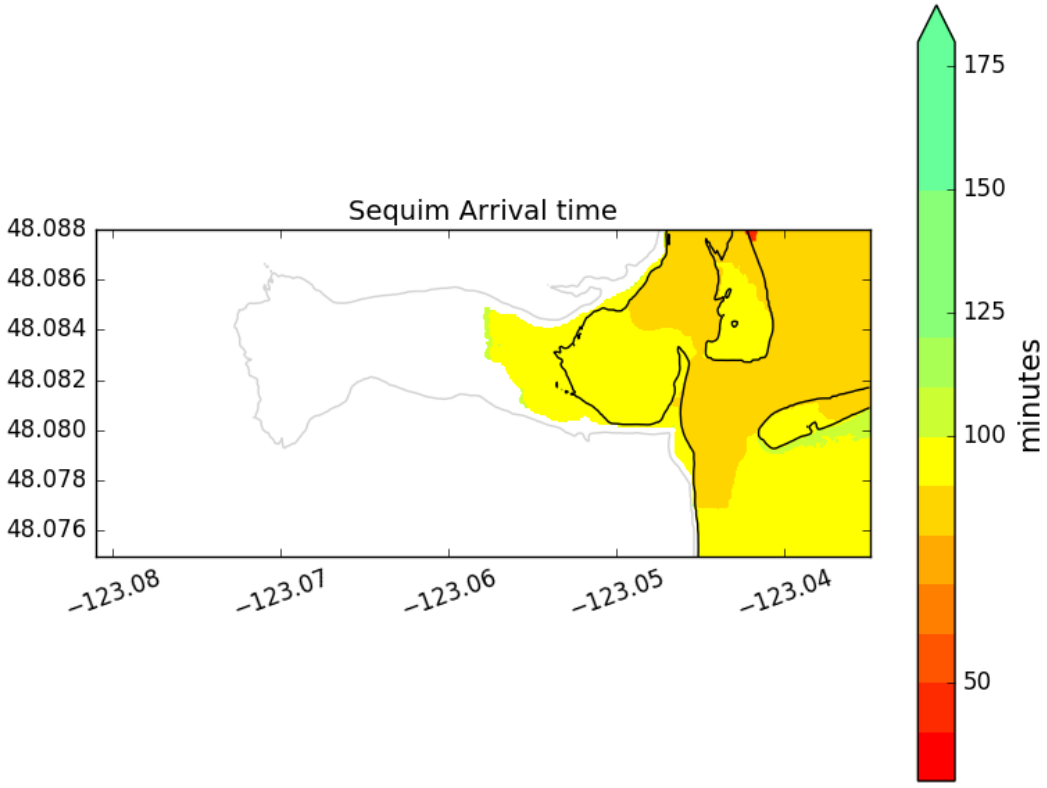

Figure 15：Tsunami arrival time along the entrance of Bell Creek Valley (minutes after the earthquake).

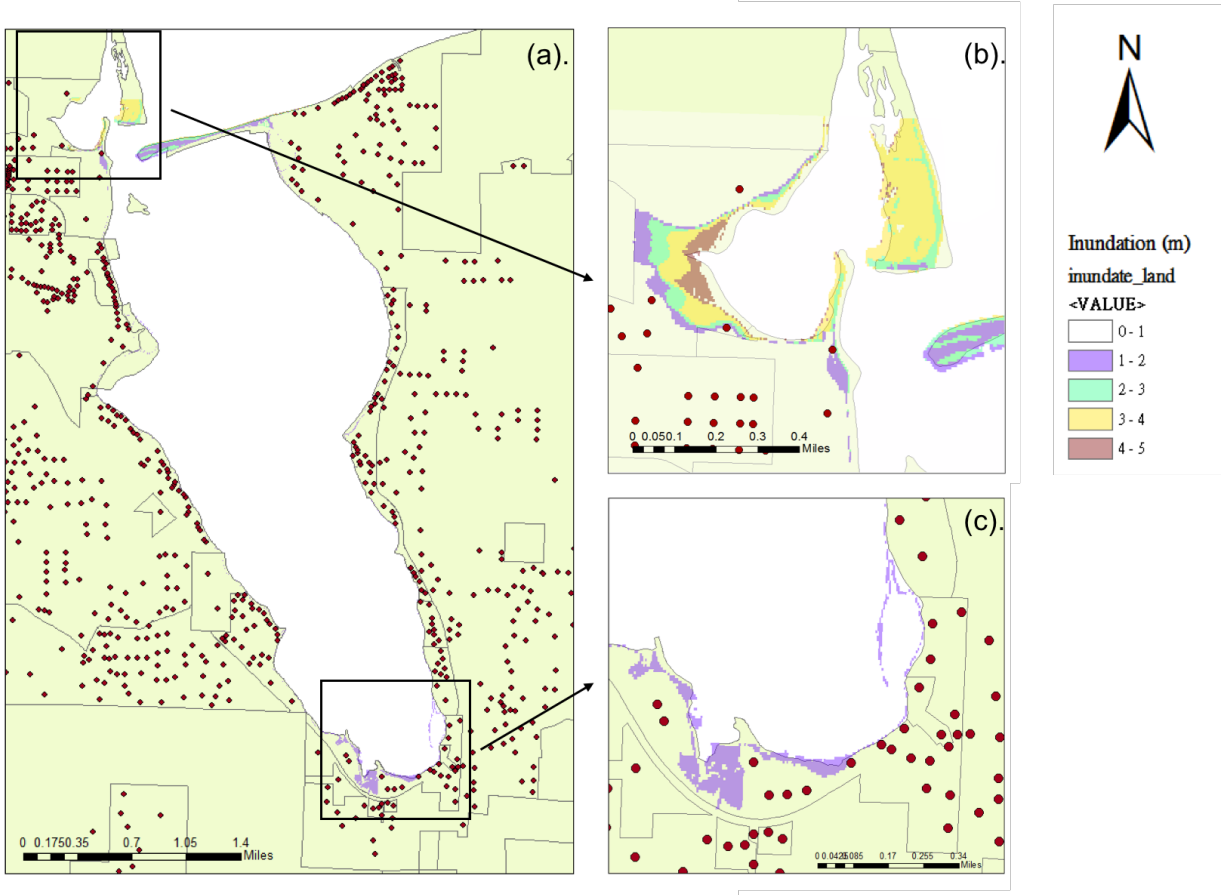

Figure 16： (a). GIS analysis of tsunami inundation in Sequim Bay. (b). Inset showing tsunami inundation in the entrance of Bell Creek valley. (c). Inset showing inundation in the southern end of the Sequim Bau. The red dots represent the location of buildings in the building inventory.

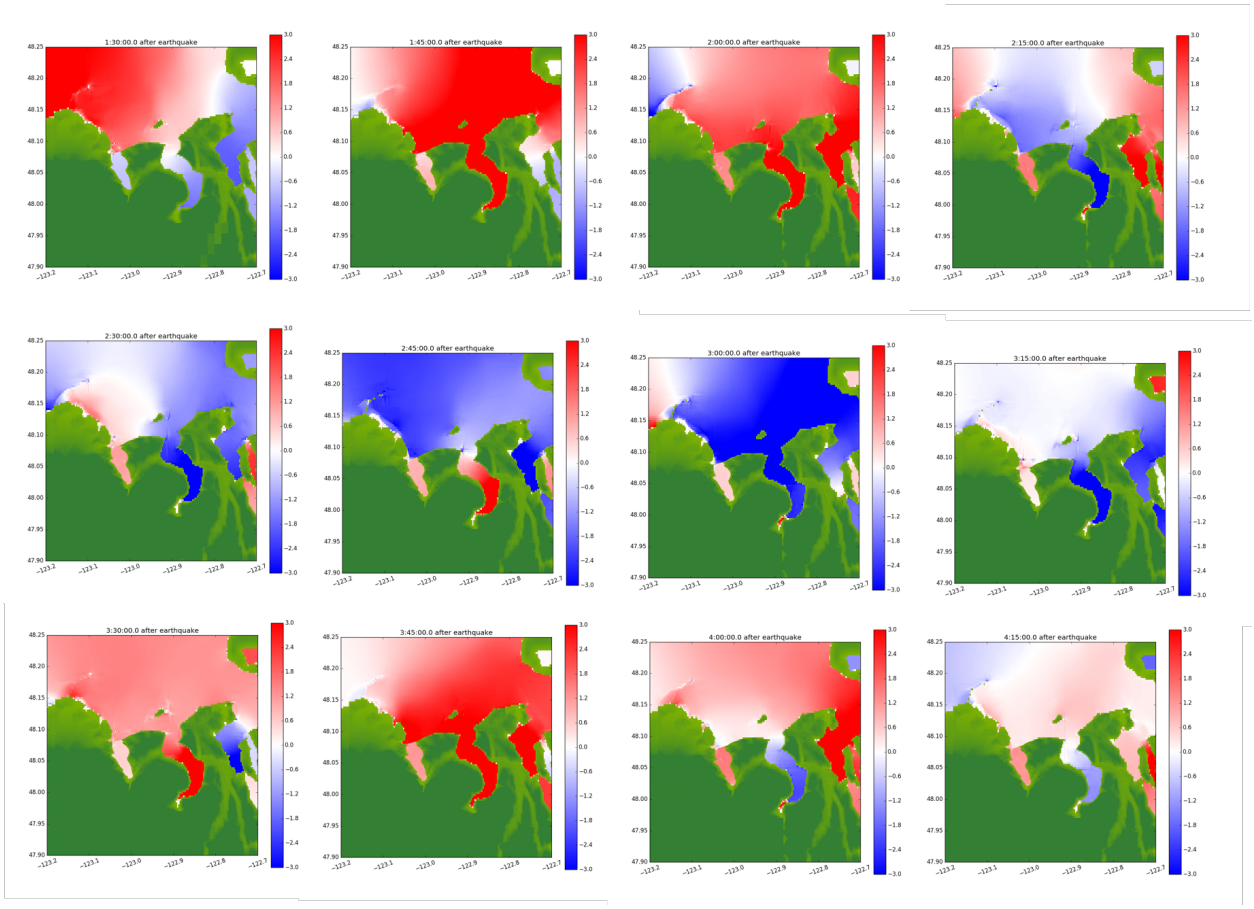

Figure 17：Tsunami propagation in Sequim Bay and Discovery Bay. Color bar as in Fig. 6.